Amiloride, an old diuretic drug, is a potential therapeutic agent for multiple myeloma

Elizabeta A. Rojas[1,3], Luis Antonio Corchete[1,2,3], Laura San-Segundo[1,3], Juan F. Martínez-Blanch[5], Francisco M. Codoñer[5], Teresa Paíno[1,3], Noemí Puig[1,2,3], Ramón García-Sanz[1,2,3], María Victoria Mateos[1,2,3], Enrique M. Ocio[1,2,3], Irena Misiewicz-Krzeminska[1,3,4]* and Norma C. Gutiérrez[1,2,3]*

[1]Cancer Research Center-IBMCC (USAL-CSIC), Salamanca, Spain; [2]Hematology Department, University Hospital of Salamanca, Spain; [3]Institute of Biomedical Research of Salamanca (IBSAL), Salamanca, Spain; [4]National Medicines Institute, Warsaw, Poland; [5]Lifesequencing S.L., Valencia, Spain.

*These authors contributed equally to this work.

Running title: Anti-myeloma activity of amiloride

Keywords: Multiple myeloma, amiloride, alternative splicing, *TP53*, spliceosome, RNA-Seq.

Correspondence: Norma C. Gutiérrez, Department of Hematology, University Hospital of Salamanca, Paseo San Vicente, 58-182, Salamanca, 37007, Spain. Phone: +34 923291384, Fax: +34 923294624, e-mail: normagu@usal.es

Financial support: This study was partially supported by the Instituto de Salud Carlos III-Cofinanciación with funding from FEDER (PI13/00111 and PI16/01074), Asociación Española Contra el Cáncer (AECC, GCB120981SAN), Gerencia Regional de Salud, Junta de Castilla y León (BIO/SA57/13 and BIO/SA22/15), and the INNOCAMPUS Program (CEI10-1-0010). IMK was supported by a Black Swan Research Initiative® grant from the International Myeloma Foundation. LAC was supported by a grant from the Fundación Española de Hematología y Hemoterapia.

Text word count: 4,795

Abstract word count: 250

Reference count: 50

Figure count: 6

Supplemental information: 1

Abstract

Purpose: The search for new drugs that control the continuous relapses of multiple myeloma (MM) is still required. Here, we report for the first time the potent anti-myeloma activity of amiloride, an old potassium-sparing diuretic approved for the treatment of hypertension and edema due to heart failure.

Experimental Design: Myeloma cell lines and primary samples were used to evaluate cytotoxicity of amiloride. *In vivo* studies were carried out in a xenograft mouse model. The mechanisms of action were investigated using RNA-Seq experiments, qRT-PCR, immunoblotting and immunofluorescence assays.

Results: Amiloride-induced apoptosis was observed in a broad panel of MM cell lines and in a xenograft mouse model. Moreover, amiloride also had a synergistic effect when combined with dexamethasone, melphalan, lenalidomide and pomalidomide. RNA-Seq experiments showed that amiloride not only significantly altered the level of transcript isoforms and alternative splicing events, but also deregulated the spliceosomal machinery. Additionally, disruption of the splicing machinery in immunofluorescence studies was associated with the inhibition of myeloma cell viability after amiloride exposure. Although amiloride was able to induce apoptosis in myeloma cells lacking p53 expression, activation of p53 signaling was observed in wild-type and mutated *TP53* cells after amiloride exposure. On the other hand, we did not find a significant systemic toxicity in mice treated with amiloride.

Conclusions: Overall, our results demonstrate the anti-myeloma activity of amiloride and provide a mechanistic rationale for its use as an alternative treatment option for relapsed MM patients, especially those with 17p deletion or *TP53* mutations that are resistant to current therapies.

Statement of translational relevance

The investigation of novel therapeutic agents is needed to manage the multiple relapses arising from resistant clones in multiple myeloma. In this study, we demonstrate for the first time the anti-myeloma activity of amiloride, a very well-known drug used in the treatment of hypokalemia, hypertension and edema. This finding together with the manageable toxicity profile of amiloride provide the rationale for conducting clinical trials that support the repositioning of this old drug for the treatment of MM. Moreover, our results showed that MM cells either with WT or mutated *TP53* were highly sensitive to amiloride, which makes this drug an attractive candidate for high-risk myeloma patients with *TP53* abnormalities.

Introduction

Despite improvements in the survival of multiple myeloma (MM) patients thanks to the introduction of novel therapeutic agents (1,2), it remains an incurable disease (3). MM initially responds to chemotherapy but relapse and chemoresistance usually occur (4), so subsequent recurrences are part of its natural history. Therefore, the search for new drugs that control the disease continues to be required.

Great efforts to develop new agents against MM have been made in recent years, to the extent that a wide array of new agents with different mechanisms of action have recently been approved. These include new monoclonal antibodies, proteasome inhibitors, immunomodulatory drugs and histone deacetylase inhibitors, among others (5). However, their approval processes required several years of research and major investment. An interesting alternative by which this long process might be shortened is the drug-repositioning approach, which involves using old drugs approved for noncancerous diseases (6). One of the advantages of this strategy is that the pharmacokinetic and pharmacodynamic properties and toxicity profiles tend to be well known. The diuretic drug, amiloride, is one such agent.

Amiloride is a potassium-sparing diuretic that has been employed clinically for more than three decades in the treatment of hypokalemia, hypertension, edema and congestive heart failure (7). Some studies demonstrated its significant anti-tumor and anti-metastasis activities that were initially associated with the inhibition of Na^+/H^+ exchangers (8). Recently, amiloride was found to modify alternative splicing (AS) in various human cancer cells (9). Pre-mRNA alternative splicing is a highly regulated process, and numerous studies have demonstrated its aberrations to be associated with cancer, tumor progression and metastasis. This mechanism has recently gained attention as a potential therapeutic target for cancer due to the differential splicing patterns identified in tumor cells and metastatic tumor populations (10–14).

In this study, we evaluated for the first time the anti-myeloma (anti-MM) effect of amiloride using *in vitro*, *ex vivo* and *in vivo* models. We found that amiloride had potent activity against a broad panel of MM cell lines regardless of *TP53* status. In addition, RNA-Seq experiments showed a strong alteration of spliceosome functionality. These encouraging findings, in conjunction with the manageable toxicity profiles of amiloride, provide a framework for evaluating its utility in clinical trials.

Methods

Reagents and MM cells

The human myeloma cell lines, NCI-H929, MM1S, MM1R and U266 were acquired from ATCC (American Type Culture Collection), RPMI-8226, KMS12-BM, KMS12-PE and JJN3 from DMSZ (Deuthche Sammlung von Mikroorganismen and Zellkulturen). RPMI-LR5 cell line was kindly provided by Dr. W.S. Dalton (Moffitt Cancer Center, Tampa, FL, USA). All cell lines were cultured in RPMI 1640 medium supplemented with 10% fetal bovine serum and antibiotics (Gibco). Cells were routinely checked for the presence of mycoplasma with MycoAlert kit (Lonza). Cell line identity was confirmed periodically by STR analysis with PowerPlex 16 HS System kit (Promega) and online STR matching analysis (www.dsmz.de/fp/cgi-bin/str.html). All MM samples from patients and cells from healthy donors were cultured in AIMV™ medium supplemented with 20% fetal bovine serum (Thermo Fisher). CD138+ plasma cells from bone marrow (BM) samples of 8 patients with MM were isolated using an autoMACS separation system (Miltenyi-Biotec, Auburn, CA, USA). Clinical information of the patients included in the study is summarized in Supplementary Material.

Amiloride and melphalan were purchased from Sigma-Aldrich (St Louis, MO, USA), bortezomib was from LC Laboratories (Woburn, MA, USA), dexamethasone was from Merck KGaA (Darmstadt, Germany), and lenalidomide and pomalidomide from Selleckchem (Houston, TX, USA). All MM patients as well as healthy donors involved in the study provided written informed consent in accordance with the Helsinki Declaration. The research ethics committee of the University Hospital of Salamanca approved the study.

Cell viability assays

Cell viability and proliferation were evaluated using CellTiter-Glo® (Promega) and 3 (4,5-dimethylthiazol-2-yl)-2,5-diphenyltetrazolium bromide (MTT) colorimetric assay (Sigma-

Aldrich), respectively, as previously described (15,16). Synergism between amiloride and other drugs was evaluated with Calcusyn software (Biosoft, Ferguson, MO, USA) (17) (Supplementary Material).

Apoptosis and cell cycle assays

Apoptosis using annexin V-FITC/propidium iodide (PI) double staining, mitochondrial membrane depolarization using DiIC1(5) (Immunostep) and cell cycle analysis, were performed by flow cytometry using Infinicyt software (Cytognos S.L., Salamanca, Spain), as previously described (15). Caspases 3/7, 8 and 9 activities were evaluated by Caspase Glo® 3/7, Caspase-Glo® 8 and Caspase-Glo® 9 assays (Promega), respectively, according to the manufacturer's protocol.

***Ex vivo* analysis of cytotoxicity in freshly total bone marrow cells**

The experiments with patient´s cells were performed in total BM samples from patients with MM. Immediately after extraction, total BM samples were lysed with ammonium chloride to remove red blood cells (erythrocytes); the remaining white blood cells were maintained for 48 hours in AIMV™ medium supplemented with 20% fetal bovine serum (Thermo Fisher) in absence or presence of different concentrations of amiloride. Then, the activity of amiloride was investigated on plasma cells (PCs) and on the main BM cell populations separately. To evaluate the cytotoxicity of amiloride on PCs, samples were analyzed using Annexin V (Immunostep) in combination with three markers that allowed for the identification of pathological PCs present in the sample. With that aim, we used a fix combination of two monoclonal antibodies (CD38 and CD45) plus a third one, chosen depending on the specific phenotype of each patient´s clonal plasma cells (usually CD56 or CD19). The cells were incubated for 15 minutes at room temperature in the dark. A total of 500,000 cells were acquired on a FACSCanto II flow cytometer (BD Biosciences). Finally, apoptosis was analyzed in pathological PCs (gated on CD38++ and CD56+/- or

CD19+/- and FSC/SSC) using the Infinicyt software. Annexin V positive events among the target populations were considered apoptotic cells.

Amiloride cytotoxicity on the other BM cell populations, that is B and T lymphocytes, NK cells and granulocytes, was assessed with the same aforementioned protocol described, but including a panel of 5 antibodies in combination with Annexin V to identify T lymphocytes ($CD3^+$), B lymphocytes ($CD19^+$), NK cells ($CD56^+/CD3^-$) and granulocytes ($SSC^{high}/CD45+^{dim}$). Among each of these populations separately, we identified as apoptotic the percentage being Annexin V positive using the Infinicyt software.

MM xenograft murine model

All animal experiments were performed according to the institutional guidelines and the protocol previously approved by the ethical committee of the University of Salamanca. For the human subcutaneous plasmacytoma model, 65 CB17-SCID mice (The Jackson Laboratory, Bar Harbor, ME, USA) were subcutaneously inoculated into the right flank with $3x10^6$ MM1S cells in 100 µL of RPMI-1640 medium and 100 µL of Matrigel (BD Biosciences, San Jose, CA, USA). Treatment was initiated immediately after tumor cell inoculation and mice were randomized to the following treatment cohorts, each of five animals: vehicle-alone PBS (C); amiloride, 10 mg/kg (A10); amiloride, 15 mg/kg (A15); dexamethasone, 0.5 mg/kg (D); melphalan, 2.5 mg/kg (M), dexamethasone + melphalan (DM); dexamethasone + amiloride, 10 mg/kg (DA10); melphalan + amiloride, 10 mg/kg (MA10); dexamethasone + melphalan + amiloride, 10 mg/kg (DMA10); dexamethasone + amiloride, 15 mg/kg (DA15); melphalan + amiloride, 15 mg/kg (MA15); and dexamethasone + melphalan + amiloride, 15 mg/kg (DMA15). Amiloride was administered orally daily, and dexamethasone and melphalan intraperitoneally (i.p.) two days a week. Tumor burden estimation and toxicity monitoring were performed as described previously (18).

To estimate survival, mice were sacrificed when the diameter of their tumor reached 2 cm or when they became moribund. Time to endpoint (TTE) was estimated from the day of treatment initiation. For *in vivo* mechanistic studies, six and four mice, respectively, were subcutaneously inoculated in the right flank with $3x10^6$ MM1S cells and $3x10^6$ RPMI cells. When the tumor attained a large volume, mice were randomized to receive the vehicle-alone PBS (control group) or amiloride (20 mg/kg) orally for two consecutive days. On the third day, mice were sacrificed and the tumors retrieved for analysis.

RNA sequencing

Poly A^+ RNA from KMS12-BM and JJN3 cells untreated or treated with amiloride (0.1 mM and 0.4 mM, respectively) for 24 h was isolated and prepared for RNA-Seq. Libraries were constructed following a TruSeq Stranded mRNA Sample Preparation Guide (Illumina). The final cDNA library was sequenced using Illumina HiSeq™ 2500 in combination of 100 Paired-End at Lifesequencing S.L. (Valencia, Spain) (Supplementary Material).

RNA sequencing analysis

Paired-end FASTQ files for 12 samples were used in the RNA-Seq analyses. We analyzed the data in three stages: gene expression, isoform level and splicing events. First, in the analysis of differential expression at the gene level, the genes were considered to be differentially expressed for an absolute n-fold change (FC) of ≥ 2 and a false discovery rate (FDR) of < 0.05. Second, in the analysis of isoform level, we focused on the isoforms with an absolute value of FC ≥ 2 and that corresponded to genes without altered total expression. The criteria used to assign genes as “no-change” were FDR > 0.05 and an absolute value of FC < 2, when the DESeq2 package was applied. Third, differential alternative splicing events were detected using rMATS version 3.0.9(19), classifying these events into five major types of pattern: skipped exon (SE), alternative 5' splice site (A5SS), alternative 3' splice site (A3SS), mutually exclusive exons (MXEs) and retained introns (RIs). rMATS also calculates the difference in the ratio of these events between two

conditions, and produces an estimate of the FDR. Finally, all the enrichment analyses were conducted using the Webgestalt web tool (20), employing the Gene Ontology and KEGG databases as data sources. The dataset is available at the Gene Expression Omnibus (GEO) repository (http://www.ncbi.nlm.nih.gov/geo) under the accession number GSE95077.

Further details are provided in the Supplementary Material.

RNA extraction and quantitative real-time PCR (qRT-PCR) analysis

RNA was extracted using the RNeasy Plus Mini kit (Qiagen). The RNA integrity was assessed with an Agilent 2100 Bioanalyzer (Agilent Technologies). Total RNA (1 µg) was reverse-transcribed to cDNA using High-Capacity cDNA Reverse Transcription Kit (Applied Biosystems). Gene expression was quantified by TaqMan qRT-PCR mRNA assays (Applied Biosystems) and normalized relative to 18S5 using the 2-ΔCt method.

Immunoblotting and immunofluorescence analysis

Western blot (WB) methods and the preparation of protein lysates have been described elsewhere (15). The sources of the monoclonal antibodies are described in the Supplementary Material.

For immunofluorescence, cells were fixed in 4% paraformaldehyde, permeabilized with 0.25% Triton X-100/PBS, stained with primary mouse anti-SC35 (Abcam) and goat anti-mouse IgG (H+L) secondary antibody, Alexa Fluor® 488 conjugate (Thermo Fisher). Fluorescence was measured under a Leica confocal microscope.

Statistical analysis

All statistical analyses were carried out with IBM SPSS Statistics 22.0 (IBM Corp., Armonk, NY, USA) and the Simfit package (W.G. Bardsley, University of Manchester, Manchester, UK; v7.0.9 Academic 32-bit, http://www.simfit.org.uk/). *p* values were corrected for multiple testing using the FDR, with values of < 0.05 being considered to be statistically significant. Differences in the *in vitro* experiments are expressed as the mean ± standard deviation

(SD) of at least three determinations and were assessed by the two-sided Student's *t* test or the Mann-Whitney *U* test. Differences in tumor volumes between groups were evaluated fitting an exponential regression model and the regression parameters were compared using a *t*-test for unequal variances. Survival curves were plotted using the Kaplan-Meier method, and compared using the log-rank test.

Results

Amiloride is cytotoxic for MM and potentiates the efficacy of various anti-myeloma agents.

Amiloride exhibited potent *in vitro* anti-MM activity in a dose- and time-dependent manner, as demonstrated in a panel of seven myeloma cell lines with a wide range of cytogenetic abnormalities and p53 status (Supplementary Table 1 and Supplementary Fig. S1A). The viability was significantly reduced in both the *TP53* wild-type (WT) (H929, MM1S) and the mutated *TP53* cell lines (KMS12-BM, KMS12-PE, U-266 and RPMI-8226) after exposure to amiloride ($p < 0.01$) (Fig. 1A), although viability reduction in the p53-null cell line JJN3 required a higher dose and a longer time course ($p < 0.01$). The anti-MM effect of amiloride was also observed in melphalan- and dexamethasone-resistant cell lines, RPMI-LR5 and MM1R, respectively (Supplementary Fig. S2A).

In the *ex vivo* study using BM cells from 10 patients with MM (six newly-diagnosed and four relapsed/refractory), we observed significant apoptosis induction in plasma cells, even in three patients bearing deletion of 17p, with minor cytotoxicity toward B and T lymphocytes, NK cells and neutrophils (Fig. 1B). Myeloma cell cytotoxicity of amiloride was also confirmed on isolated CD138+ plasma cells from eight MM patients (Supplementary Fig. S1B). Interestingly, amiloride did not induced cytotoxicity on normal plasma cells from healthy donors (Supplementary Fig. S1C).

Next, we evaluated the cytotoxicity of double combinations of amiloride with melphalan and dexamethasone, employing a constant ratio between them. Subsequent isobologram analysis revealed a combination index (CI) in the synergistic range for the double combinations of amiloride with dexamethasone or melphalan, ranging from 0.2 to 0.8, depending on the doses and cell lines used (Fig. 1C and Supplementary Fig. S2B). Furthermore, amiloride overcame the melphalan and dexamethasone resistance of RPMI-LR5 and MM1R, respectively (Supplementary Fig. S2C, D). Amiloride was also combined

with new agents such as lenalidomide, pomalidomide and bortezomib. A significant synergism was observed between amiloride and lenalidomide or pomalidomide plus dexamethasone (Fig. 1D, E). By contrast, the combination of amiloride with bortezomib was antagonistic in all cell lines tested (Supplementary Fig. S2E).

To test whether amiloride was able to inhibit the protective effect of the BM microenvironment, MM1S-luc cells were cocultured with mesenchymal stem cells (MSCs) from six MM patients and treated with increasing concentrations of amiloride for 48 hours. Despite the proliferative advantage to MM cells conferred by MSCs, amiloride abrogated the protective effect conferring by MSCs. In contrast, MSCs were resistant to the cytotoxic effect of amiloride (Supplementary Fig. S3).

Amiloride induces apoptosis and enhances mitochondrial depolarization

In order to elucidate the mechanisms leading to the decrease of cell growth induced by amiloride, we analyzed cell cycle and apoptosis in MM cell lines treated with increasing concentrations of the drug (0.1-1.0 mM). Amiloride induced significant apoptosis after 24 and 48 h in H929, KMS12-BM and JJN3 cell lines (Fig. 2A and Supplementary Fig. S4A), as well as in MM1S, U-266 and RPMI cell lines after 48 h (Supplementary Fig. S4B). The apoptosis induction was dose-dependent in all cell lines, with the highest levels in the KMS12-BM cell line, even at 0.1 mM after 24 h of treatment (Fig. 2A). It is of particular note that the apoptosis induced by amiloride was also observed in cells with del(17p) or *TP53* mutations (JJN3 and KMS12-BM, respectively). No significant effect of amiloride on cell cycle was observed (Supplementary Fig. S5).

To evaluate the involvement of mitochondria in cell death, the membrane potential ($\Delta\Psi_m$) was measured. Amiloride caused a decrease in $\Delta\Psi_m$, particularly significantly in KMS12-BM, H929 and RPMI-8226 cells (Fig. 2B and Supplementary Fig. 6). Using a luminescent-proteolytic assay, we observed that the caspases 3/7, 8 and 9 were significantly activated in all the cell lines tested (Fig. 2C and Supplementary Fig. S7A). The involvement of a

caspase-independent mechanism was also observed, as Z-VAD-FMK, a pan-caspase inhibitor, was able to inhibit caspase 3/7 activity, but unable to inhibit apoptosis induced by amiloride (Supplementary Fig. S7B).

***In vivo* anti-myeloma efficacy of amiloride**

We evaluated the *in vivo* efficacy of amiloride (A) in monotherapy and in combination with melphalan (M) and dexamethasone (D). Since to the best of our knowledge there are no data concerning the anti-tumor efficacy of amiloride in the animal model used here, we evaluated two doses of amiloride (10 mg/kg and 15 mg/kg). Treatment of MM1S-inoculated CB17-SCID mice with a double or triple combination of A (regardless of the A dose applied), together with D and/or M, enhanced tumor growth inhibition, although the differences were only statistically significant for the combinations DA10, DA15 and DMA15 (Fig. 3A and Supplementary Fig. S8A). With respect to survival, we observed a significant improvement in TTE in the group of mice treated with the double combinations, DA10 and MA10, and the triple combination, DMA10, compared with the D, M and DM groups, respectively ($p < 0.05$) (Fig. 3B). The mice treated with the triple combination DMA10 had a median overall survival (OS) of 115 days compared with 99 days for the combination DM ($p < 0.05$) (Fig. 3B). The double combinations, DA15 and MA15, also showed a statistically significant benefit ($p < 0.01$) in terms of OS compared with the single drugs (Supplementary Fig. S8B). The triple combination DMA15 also had a longer OS (median, 110 days) than the double combination DM (median, 99 days), although the difference was not statistically significant ($p = 0.053$) (Supplementary Fig. S8B). No significant toxicity, measured as body weight loss, was observed in the mice receiving combinations with amiloride (Supplementary Fig. S8C).

Amiloride induces gene and transcript isoforms expression changes

To determine the molecular basis of the anti-myeloma activity of amiloride, we performed RNA-Seq analysis in KMS12-BM and JJN3 cell lines, the most and the least sensitive,

respectively, at the beginning of apoptosis (15 - 25% cell death, assessed by CellTiter-Glo luminescent assays) after amiloride treatment. The study design is shown in Supplementary Fig. S9. RNA-Seq data were analyzed at three levels: gene, isoform and splicing events. Although there were clearly more deregulated genes in KMS12-BM (almost 5,000) than in the JJN3 cell line (almost 1,000) (Fig. 4A), significant enrichment of functional categories, such as metabolic, MAPK and Jak-STAT signaling pathways, and endocytosis (Supplementary Fig. S10A), were found among the genes deregulated in both cell lines after amiloride treatment. The analysis of differential expression at the isoform level identified a similar number of deregulated transcript isoforms (over 15,000) in both cell lines (Supplementary Fig. S10B).

Next, we focused our analysis on those genes with a total expression that was not differentially modified after amiloride treatment, but whose transcript isoforms were differentially expressed. We found a considerable number of genes that were significantly deregulated at the isoform but not the gene level in both cell lines (Fig. 4B). Among the most significantly enriched pathways with deregulated transcript isoforms, in both cell lines, were those of the spliceosome, apoptosis, metabolic pathways, and those associated with protein-processing in ER, oxidative phosphorylation, cell cycle, RNA transport and endocytosis (Fig. 4C). Transcript isoforms belonging to different components of the spliceosome and that are involved in the assembly and regulation of the spliceosomal machinery were significantly deregulated after amiloride treatment (Supplementary Table 3). For example, the transcript ENST00000269601, which encodes the canonical protein TXNL4A, is upregulated in myeloma cells treated with amiloride, whereas the transcript ENST00000588162, which encodes a smaller protein, was only expressed in untreated cells. Notably, the p53 pathway was only highly enriched in p53-expressing cell line, KMS12-BM, but not in the p53-null cell line, JJN3 (Fig. 4C and Supplementary Table 4).

Finally, using Multivariate Analysis of Transcript Splicing software we identified thousands of alternative splicing (AS) events in both cell lines after amiloride exposure (Fig. 4D). Most of the significant AS events (FDR < 0.05) involved genes whose total expression was not modified by amiloride, indicating that the deregulation of alternative splicing could be a specific mechanism of action of amiloride. The most common AS event in both cell lines was the SE, which is the most common splice event in mammalian pre-mRNAs.

Amiloride modulates alternative splicing machinery

Given that RNA-Seq results showed deregulation of alternative splicing and spliceosome components in myeloma cells, we next evaluated whether the anti-myeloma effect of amiloride was associated with modulation of the splicing machinery. The immunofluorescent staining for the SR (serine/arginine-rich) protein SC35 demonstrated the amiloride-induced modulation of the splicing machinery in myeloma cells with distinct *TP53* status. Thus, the modulation of the splicing machinery was accompanied by a reduction in cell viability in the H929 and JJN3 cell lines (Fig. 5). In both settings, the number of speckles was reduced but the remaining speckles increased in size and intensity. This finding was confirmed *in vivo* (Supplementary Fig. S11A) using xenografts inoculated with other MM cell lines. Structural changes of the nuclear speckles induced by amiloride were also observed in CD138+ cells from one newly-diagnosed MM patient (Supplementary Fig S11B). Additionally, mRNA levels of the spliceosome components (SNRNP27, SRSF4, SF3B1, LSM3, LSM14A, PRPF3 and PRPF4) were significantly overexpressed in myeloma cells from patients after amiloride treatment (Supplementary Fig S11C). Altogether, these results suggest the potential association between the anti-myeloma activity of amiloride and the modulation of spliceosomal machinery.

Anti-myeloma activity of amiloride is associated with functional p53 signaling

Our results showed that MM cells either with WT or mutated *TP53* were highly sensitive to amiloride, although higher doses and longer exposure to amiloride were required for p53-

null cells. Moreover, pathway enrichment analysis from RNA-Seq data in mutated *TP53* cells revealed a subset of deregulated transcript isoforms involved in the p53 pathway. These findings suggest an activation of p53 signaling pathway in MM cells after treatment with amiloride. To test this hypothesis, we used qRT-PCR to measure the expression of p53 targets, such as *BAK1*, *BBC3*, *TNFRSF10B*, *FAS*, *CDKN1B* and *CDKN1A* in MM cell lines with different *TP53* status. We observed a normal functional p53 response in the WT/WT cell line (MM1S), whereas p53 signaling was abrogated in JJN3 cells with no basal p53 expression (Fig. 6A). Interestingly, the mutated *TP53* cell lines (KMS12-BM and U-266) also showed overexpression of p53 targets. Similar results were found by RNA-Seq data analysis (Supplementary Fig. S12). The activation of p53 signaling pathway was confirmed in CD138+ cells from eight MM patients after treatment with amiloride (Supplementary Fig. S13)

The cell lines with mutated *TP53* showed deregulation of p53 targets after treatment with amiloride, so we decided to confirm the involvement of p53 in amiloride-induced cytotoxicity of MM cells. The functionality of p53 signaling pathway in mutated *TP53* cell lines was confirmed using p53 activity inhibitors: pifithrin-α (PFTα), a reversible inhibitor of p53-mediated apoptosis and p53-dependent gene transcription(21), and pifithrin-μ (PFTμ), an inhibitor of the p53-Bcl-xL interaction that directly inhibits p53 binding to mitochondria (22). Amiloride cytotoxicity was reduced in WT and mutated *TP53* MM cell lines when used with p53 inhibitors. As expected, the inhibitors had no effect on the death of JJN3 cells, which lack p53 expression (Fig. 6B). These results imply that p53 signaling has an important role in amiloride-induced apoptosis of MM cells that express either WT or mutated *TP53*. On the other hand, the involvement of a mechanism other than p53 signaling activation would explain the anti-myeloma effect of amiloride on p53-null cells.

Discussion

In this study, we demonstrate for the first time the anti-myeloma activity of amiloride, an anti-hypertensive drug, through two novel mechanisms of action, spliceosome deregulation and p53 signaling pathway activation. Initially, we observed potent *in vitro* anti-myeloma activity of amiloride, both in *TP53* wild-type and mutated *TP53* cells. Even in p53-null cells, viability was reduced by using higher doses and longer exposures. The *ex vivo* study of myeloma cells from patients indicated that amiloride induced cytotoxicity in plasma cells, including three cases bearing deletion of 17p, whereas viability of other BM cell populations was not affected. Furthermore, amiloride in combination with dexamethasone and melphalan was clearly synergic *in vitro*. A synergic effect was also observed when amiloride was combined with lenalidomide or pomalidomide plus dexamethasone. In this context, amiloride has been described as potentiating synergistically the anti-proliferative effect of other drugs like imatinib, the frontline therapy for patients with chronic myeloid leukemia (CML) (23,24). However, we did not find synergism between amiloride and bortezomib, which could limit the use of amiloride in bortezomib-based induction regimens.

The induction of apoptosis by amiloride in CML was accompanied by the increase in levels of caspases 9 and 3. Our results showed that the apoptosis induced by amiloride was mediated by both caspase-dependent and caspase-independent mechanisms, which is consistent with other studies in glioblastoma and breast tumor cells (25–27). Moreover, we observed increased survival of mice bearing human subcutaneous plasmacytomas treated with double or triple combinations including amiloride compared with treatment with melphalan and/or dexamethasone.

The anti-cancer effect of amiloride has previously been described in several tumors, using *in vitro* and *in vivo* models (9,23–33). There is evidence for multiple mechanisms of action of amiloride, including TRAIL-induced cytotoxicity associated with the PI3K-Akt pathway

(24,28,30,33) and alternative splicing deregulation of apoptotic genes (9,23,28). The RNA-Seq allowed us to study its mechanism of action in myeloma cells more extensively. In fact, RNA-Seq analysis in two cell lines with distinct patterns of response to the drug, the most and the least sensitive, revealed that amiloride significantly altered the level of transcript isoforms and the alternative splicing events. It should be pointed out that the significant impact on the differential expression of isoforms from genes whose total expression was not changed. In other words, the traditional gene expression profiling would have overlooked the substantial modifications of more than 10,000 transcript isoforms by amiloride treatment. These results are consistent with the reported advantage of the analysis at the genome-wide isoform level compared with gene expression in cancer research (34,35).

One of the most significantly enriched pathways in the analysis of differentially expressed isoforms after amiloride treatment was spliceosome. We found that amiloride induced a general deregulation of spliceosomal machinery at the gene and transcript isoform levels that affected the early and late stages of spliceosome assembly and several spliceosome-associated proteins, including the catalytic steps of the splicing. These findings, together with the large quantity of total transcript isoforms modified by amiloride, prompted us to investigate further the influence of amiloride in the pre-mRNA splicing machinery. The small nuclear ribonucleoproteins (snRNPs) and splicing factors, like the SR protein family, are organized in nuclear speckles (36). The changes in protein SC35-staining speckles are used as a marker for the disruption of the splicing machinery (37–40). Upon the inhibition of the splicing machinery, the number of nuclear speckles decreases but those remaining increase in size and intensity (36,41). Using this marker, after amiloride treatment, we identified a similar pattern of nuclear speckle modifications that was associated with cell viability inhibition. This finding indicates that amiloride provokes the disruption of the splicing machinery and that this could, in turn, induce cytotoxicity.

The RNA-Seq analysis at the transcript isoform level also identified the p53 pathway as one of the most significantly enriched functional categories. Remarkably, the p53 pathway was highly overexpressed only in the cell line expressing mutated *TP53*, and not in the p53-null cell line. Additionally, upregulation of p53 targets was observed in WT and mutated *TP53* myeloma cells treated with amiloride. These results, together with the fact that the inhibition of p53 protein activity prevents amiloride-induced cell death, even in two mutated *TP53* cell lines, demonstrate that amiloride-induced apoptosis in myeloma cells is dependent on p53 activation and is independent of the mutational status of *TP53.* Apart from that, the reduction in cell viability in the amiloride-treated p53-null cell line supports the notion that other mechanisms independent of p53, such as the spliceosomal machinery disruption observed in JJN3 cell line, are involved in amiloride activity.

Amiloride has been used for many years as adjuvant treatment with thiazide diuretics in congestive heart failure and hypertension (42–45). Here, we demonstrate for the first time the therapeutic potential of amiloride in MM. The concentration of amiloride used in the *in vivo* experiments is higher than that commonly used as a potassium-sparing diuretic, suggesting that a higher dose would be needed to produce the anti-MM effect. The toxicity profile of this drug is very well known and the main side effect is hyperkalemia, which could be the main factor that limits the use of amiloride as an anti-myeloma drug. To minimize this risk, a careful electrolyte monitoring along with the co-administration of a kaliuretic agent or the use of new oral agents for the hyperkalemia treatment, such as patiromer calcium (46–48) and ZS-9 (zirconium cyclosilicate) (48–50), could be required. Moreover, attempts to develop amiloride analogues that show reduced diuretic and antikaliuretic effects retaining or enhancing anti-cancer activity are currently underway in different laboratories. On the other hand, as reported in other studies (23,32), we did not find any significant systemic toxicity in the mice treated with amiloride, and the

viability of the lymphocyte population either from MM patients or healthy donors was not affected, even at the highest dose.

Our results also revealed that the anti-myeloma activity of amiloride was mediated through spliceosome modulation and involved the p53 pathway. In fact, p53 signaling was activated after amiloride exposure, independently of the mutational status of *TP53*. On the other hand, amiloride was also able to induce apoptosis in myeloma cells that did not express p53.

In conclusion, these findings together with the possibility of combining amiloride with melphalan, dexamethasone or lenalidomide or pomalidomide, support the initiation of clinical trials including amiloride for patients with relapsed and refractory MM, particularly for those with 17p deletion or *TP53* mutations who display a poor prognosis.

Acknowledgements

The authors thank Isabel Isidro, Teresa Prieto, Vanesa Gutiérrez, Irene Aires and José Pérez for their technical assistance; Lorena González for the help with the assays of the combinations of anti-myeloma drugs; Mercedes Garayoa for the help with MSCs studies; and Phil Mason for his help in reviewing the English language of the manuscript.

Authorship Contributions

E.A.R. designed the research, performed the experiments, analyzed the data, and wrote the manuscript. L.A.C analyzed the RNA-Seq data and reviewed the statistical studies. L.S.S. performed the *in vivo* studies. J.M and F.M.C performed and analyzed RNA-Seq. T.P. contributed to synergism studies. N.P. carried out flow cytometry studies. R.G.S. and M.V.M. provided primary MM cells and contributed to the research tools. E.M.O. designed the *in vivo* studies and provided study support. I.M.K. and N.C.G. conceptualized the initial idea of the study, supervised the research project and were responsible for the final approval of the manuscript.

Disclosure of Conflicts of Interest

The authors declare no conflicts of interest.

References

1. Kumar SK, Rajkumar SV, Dispenzieri A, Lacy MQ, Hayman SR, Buadi FK, et al. Improved survival in multiple myeloma and the impact of novel therapies. Blood. 2008;111:2516–20.

2. Kumar SK, Dispenzieri A, Lacy MQ, Gertz MA, Buadi FK, Pandey S, et al. Continued improvement in survival in multiple myeloma: changes in early mortality and outcomes in older patients. Leukemia. 2014;28:1122–8.

3. Mateos M-V, Ocio EM, Paiva B, Rosiñol L, Martínez-López J, Bladé J, et al. Treatment for patients with newly diagnosed multiple myeloma in 2015. Blood Rev. 2015;29:387–403.

4. Kumar SK, Lee JH, Lahuerta JJ, Morgan G, Richardson PG, Crowley J, et al. Risk of progression and survival in multiple myeloma relapsing after therapy with IMiDs and bortezomib: a multicenter international myeloma working group study. Leukemia. 2012;26:149–57.

5. Rajan AM, Kumar S. New investigational drugs with single-agent activity in multiple myeloma. Blood Cancer J. 2016;6:e451.

6. Würth R, Thellung S, Bajetto A, Mazzanti M, Florio T, Barbieri F. Drug-repositioning opportunities for cancer therapy: novel molecular targets for known compounds. Drug Discov Today. 2016;21:190–9.

7. Tang CM, Presser F, Morad M. Amiloride selectively blocks the low threshold (T) calcium channel. Science. 1988;240:213–5.

8. Slepkov ER, Rainey JK, Sykes BD, Fliegel L. Structural and functional analysis of the Na+/H+ exchanger. Biochem J. 2007;401:623–33.

9. Chang J-G, Yang D-M, Chang W-H, Chow L-P, Chan W-L, Lin H-H, et al. Small molecule amiloride modulates oncogenic RNA alternative splicing to devitalize human cancer cells. PloS One. 2011;6:e18643.

10. Tazi J, Bakkour N, Stamm S. Alternative splicing and disease. Biochim Biophys Acta. 2009;1792:14–26.

11. Wang G-S, Cooper TA. Splicing in disease: disruption of the splicing code and the decoding machinery. Nat Rev Genet. 2007;8:749–61.

12. Cartegni L, Chew SL, Krainer AR. Listening to silence and understanding nonsense: exonic mutations that affect splicing. Nat Rev Genet. 2002;3:285–98.

13. Venables JP. Aberrant and alternative splicing in cancer. Cancer Res. 2004;64:7647–54.

14. Kim E, Goren A, Ast G. Insights into the connection between cancer and alternative splicing. Trends Genet TIG. 2008;24:7–10.

15. Misiewicz-Krzeminska I, Sarasquete ME, Quwaider D, Krzeminski P, Ticona FV, Paíno T, et al. Restoration of microRNA-214 expression reduces growth of myeloma cells through positive regulation of P53 and inhibition of DNA replication. Haematologica. 2013;98:640–8.

16. Maiso P, Carvajal-Vergara X, Ocio EM, López-Pérez R, Mateo G, Gutiérrez N, et al. The histone deacetylase inhibitor LBH589 is a potent antimyeloma agent that overcomes drug resistance. Cancer Res. 2006;66:5781–9.

17. Chou T-C. Drug combination studies and their synergy quantification using the Chou-Talalay method. Cancer Res. 2010;70:440–6.

18. Ocio EM, Vilanova D, Atadja P, Maiso P, Crusoe E, Fernández-Lázaro D, et al. In vitro and in vivo rationale for the triple combination of panobinostat (LBH589) and dexamethasone with either bortezomib or lenalidomide in multiple myeloma. Haematologica. 2010;95:794–803.

19. Shen S, Park JW, Lu Z, Lin L, Henry MD, Wu YN, et al. rMATS: robust and flexible detection of differential alternative splicing from replicate RNA-Seq data. Proc Natl Acad Sci U S A. 2014;111:E5593-5601.

20. Wang J, Duncan D, Shi Z, Zhang B. WEB-based GEne SeT AnaLysis Toolkit (WebGestalt): update 2013. Nucleic Acids Res. 2013;41:W77-83.

21. Farah IO, Begum RA, Ishaque AB. Differential protection and transactivation of P53, P21, Bcl2, PCNA, cyclin G, and MDM2 genes in rat liver and the HepG2 cell line upon exposure to pifithrin. Biomed Sci Instrum. 2007;43:116–21.

22. Hagn F, Klein C, Demmer O, Marchenko N, Vaseva A, Moll UM, et al. BclxL changes conformation upon binding to wild-type but not mutant p53 DNA binding domain. J Biol Chem. 2010;285:3439–50.

23. Chang W-H, Liu T-C, Yang W-K, Lee C-C, Lin Y-H, Chen T-Y, et al. Amiloride modulates alternative splicing in leukemic cells and resensitizes Bcr-AblT315I mutant cells to imatinib. Cancer Res. 2011;71:383–92.

24. Zheng Y, Yang H, Li T, Zhao B, Shao T, Xiang X, et al. Amiloride sensitizes human pancreatic cancer cells to erlotinib in vitro through inhibition of the PI3K/AKT signaling pathway. Acta Pharmacol Sin. 2015;36:614–26.

25. Leon LJ, Pasupuleti N, Gorin F, Carraway KL. A cell-permeant amiloride derivative induces caspase-independent, AIF-mediated programmed necrotic death of breast cancer cells. PloS One. 2013;8:e63038.

26. Hegde M, Roscoe J, Cala P, Gorin F. Amiloride kills malignant glioma cells independent of its inhibition of the sodium-hydrogen exchanger. J Pharmacol Exp Ther. 2004;310:67–74.

27. Harley W, Floyd C, Dunn T, Zhang X-D, Chen T-Y, Hegde M, et al. Dual inhibition of sodium-mediated proton and calcium efflux triggers non-apoptotic cell death in malignant gliomas. Brain Res. 2010;1363:159–69.

28. Tang J-Y, Chang H-W, Chang J-G. Modulating roles of amiloride in irradiation-induced antiproliferative effects in glioblastoma multiforme cells involving Akt phosphorylation and the alternative splicing of apoptotic genes. DNA Cell Biol. 2013;32:504–10.

29. Yang X, Wang D, Dong W, Song Z, Dou K. Suppression of Na+/H + exchanger 1 by RNA interference or amiloride inhibits human hepatoma cell line SMMC-7721 cell invasion. Med Oncol Northwood Lond Engl. 2011;28:385–90.

30. Cho Y-L, Lee K-S, Lee S-J, Namkoong S, Kim Y-M, Lee H, et al. Amiloride potentiates TRAIL-induced tumor cell apoptosis by intracellular acidification-dependent Akt inactivation. Biochem Biophys Res Commun. 2005;326:752–8.

31. Sparks RL, Pool TB, Smith NK, Cameron IL. Effects of amiloride on tumor growth and intracellular element content of tumor cells in vivo. Cancer Res. 1983;43:73–7.

32. Matthews H, Ranson M, Kelso MJ. Anti-tumour/metastasis effects of the potassium-sparing diuretic amiloride: an orally active anti-cancer drug waiting for its call-of-duty? Int J Cancer. 2011;129:2051–61.

33. Kim KM, Lee YJ. Amiloride augments TRAIL-induced apoptotic death by inhibiting phosphorylation of kinases and phosphatases associated with the P13K-Akt pathway. Oncogene. 2005;24:355–66.

34. Zhang C, Li H-R, Fan J-B, Wang-Rodriguez J, Downs T, Fu X-D, et al. Profiling alternatively spliced mRNA isoforms for prostate cancer classification. BMC Bioinformatics. 2006;7:202.

35. Zhang Z, Pal S, Bi Y, Tchou J, Davuluri RV. Isoform level expression profiles provide better cancer signatures than gene level expression profiles. Genome Med. 2013;5:33.

36. Shepard PJ, Hertel KJ. The SR protein family. Genome Biol. 2009;10:242.

37. Kotake Y, Sagane K, Owa T, Mimori-Kiyosue Y, Shimizu H, Uesugi M, et al. Splicing factor SF3b as a target of the antitumor natural product pladienolide. Nat Chem Biol. 2007;3:570–5.

38. Kaida D, Motoyoshi H, Tashiro E, Nojima T, Hagiwara M, Ishigami K, et al. Spliceostatin A targets SF3b and inhibits both splicing and nuclear retention of pre-mRNA. Nat Chem Biol. 2007;3:576–83.

39. Allende-Vega N, Dayal S, Agarwala U, Sparks A, Bourdon J-C, Saville MK. p53 is activated in response to disruption of the pre-mRNA splicing machinery. Oncogene. 2013;32:1–14.

40. Ghosh G, Adams JA. Phosphorylation mechanism and structure of serine-arginine protein kinases. FEBS J. 2011;278:587–97.

41. Spector DL, Lamond AI. Nuclear speckles. Cold Spring Harb Perspect Biol. 2011;3.

42. Fuchs SC, Poli-de-Figueiredo CE, Figueiredo Neto JA, Scala LCN, Whelton PK, Mosele F, et al. Effectiveness of Chlorthalidone Plus Amiloride for the Prevention of Hypertension: The PREVER-Prevention Randomized Clinical Trial. J Am Heart Assoc. 2016;5.

43. Andersen H, Hansen PBL, Bistrup C, Nielsen F, Henriksen JE, Jensen BL. Significant natriuretic and antihypertensive action of the epithelial sodium channel blocker amiloride in diabetic patients with and without nephropathy. J Hypertens. 2016;34:1621–9.

44. Oxlund CS, Buhl KB, Jacobsen IA, Hansen MR, Gram J, Henriksen JE, et al. Amiloride lowers blood pressure and attenuates urine plasminogen activation in patients with treatment-resistant hypertension. J Am Soc Hypertens JASH. 2014;8:872–81.

45. Fuchs FD, Scala LCN, Vilela-Martin JF, de Mello RB, Mosele F, Whelton PK, et al. Effectiveness of chlorthalidone/amiloride versus losartan in patients with stage I hypertension: results from the PREVER-treatment randomized trial. J Hypertens. 2016;34:798–806.

46. Weir MR, Bakris GL, Bushinsky DA, Mayo MR, Garza D, Stasiv Y, et al. Patiromer in patients with kidney disease and hyperkalemia receiving RAAS inhibitors. N Engl J Med. 2015;372:211–21.

47. Bakris GL, Pitt B, Weir MR, Freeman MW, Mayo MR, Garza D, et al. Effect of Patiromer on Serum Potassium Level in Patients With Hyperkalemia and Diabetic Kidney Disease: The AMETHYST-DN Randomized Clinical Trial. JAMA. 2015;314:151–61.

48. Henneman A, Guirguis E, Grace Y, Patel D, Shah B. Emerging therapies for the management of chronic hyperkalemia in the ambulatory care setting. Am J Health-Syst Pharm AJHP Off J Am Soc Health-Syst Pharm. 2016;73:33–44.

49. Linder KE, Krawczynski MA, Laskey D. Sodium Zirconium Cyclosilicate (ZS-9): A Novel Agent for the Treatment of Hyperkalemia. Pharmacotherapy. 2016;36:923–33.

50. Packham DK, Kosiborod M. Pharmacodynamics and pharmacokinetics of sodium zirconium cyclosilicate [ZS-9] in the treatment of hyperkalemia. Expert Opin Drug Metab Toxicol. 2016;12:567–73.

Figure Legends

Figure 1. Anti-myeloma activity of amiloride in *in vitro* and *ex vivo* studies. (A) The indicated MM cell lines were incubated with increasing concentrations of amiloride for 24, 48 and 72 h. Cell viability was analyzed by CellTiter-Glo luminescent assays. The average luminescent values of the untreated control samples were taken as 100%. Results are the means of three independent experiments. The statistically significant differences between untreated and treated cell lines were determined with Student's t-test. (B) BM cells from patients with MM, were treated *ex vivo* with increasing concentrations of amiloride for 48 h. After the incubation period, cells were stained with the combination of Annexin V-FITC and three monoclonal antibodies (CD45-PerCP-Cy5.5, CD38-APC and CD56 or CD19-PE,) for the analysis of apoptosis in plasma cells. A panel of five antibodies in combination with Annexin V was used for the analysis of apoptosis in T and B lymphocytes, NK cells and granulocytes. Results are presented as the percentage of Annexin V-positive cells. Statistically significant differences are represented as ***FDR < 0.001 and **FDR < 0.01 (Mann–Whitney U test). RPMI-8226 cell line was treated with the indicated double combinations of amiloride with melphalan or dexamethasone (C) and triple combinations with pomalidomide or lenalidomide plus dexamethasone (D, E). Cell viability was assessed by MTT assay, as represented in the graphs. The combination indexes (CIs) were calculated with the Calcusyn software. CIs of <0.3, 0.3-0.7, 0.7-0.85, 0.85-0.90, 0.90-1.10, and >1.10 indicate strong synergism, synergism, moderate synergism, slight synergism, additive effect, and antagonism, respectively. C: control; A: amiloride; D: dexamethasone; M: melphalan; P: pomalidomide; L: lenalidomide; d1, d2 and d3: drug concentrations used in the study; CR: constant ratio.

Figure 2. Amiloride induces apoptosis, activates caspases and deregulates mitochondrial potential in MM cell lines. H929, JJN3 and KMS12-BM cells were treated with increasing concentrations of amiloride for 24 h. (A) The induction of apoptosis was

analyzed by flow cytometry after annexin-V/PI staining. (B) Mitochondrial membrane depolarization was examined by flow cytometry after DilC1(5) staining. (C) The activity of caspase 8, caspase 9 and caspase 3/7 was analyzed by luminescent caspase assays. Results are expressed as the mean ± SD of three independent experiments. Statistically significant differences between untreated and treated cell lines are represented as $^{**}p < 0.01$ and $^{*}p < 0.05$ (Student's t-test).

Figure 3. The triple and double combination of dexamethasone and melphalan with amiloride displays superior anti-MM activity and improves median survival compared with single agents and double combinations in a subcutaneous plasmacytoma model. CB17-SCID mice subcutaneously inoculated with 3 x 10^6 MM1S cells in the right flank were randomized to receive vehicle, amiloride (10 mg/kg, oral, daily), dexamethasone (0.5 mg/kg, i.p., 2 days per week), melphalan (2.5 mg/kg, i.p., 2 days per week) in monotherapy and the respective double and triple combinations (n = 5/group). (A) Evolution of tumor volumes of the plasmacytomas. Statistical differences between groups were evaluated fitting an exponential regression model and the regression parameters were compared using a *t*-test for unequal variances. Bars indicate standard errors of the mean. (B) Kaplan-Meier curves representing the survival of each treatment group. Mice were sacrificed when their tumor diameters reached 2 cm or when they became moribund. Statistically significant differences were analyzed by the log-rank test, and are represented as $^{*}p < 0.05$.

Figure 4. **Amiloride induces gene and isoform expression changes and modulates alternative splicing.** RNA sequencing analysis was conducted on Poly A+ RNA from KMS12-BM and JJN3 cell lines, treated or untreated with amiloride (0.1 mM and 0.4 mM, respectively) for 24 h. (A) Distribution of differentially expressed genes induced by amiloride (overexpressed with FC ≥ 2 and FDR < 0.05; underexpressed with FC ≤ -2 and FDR < 0.05 and not deregulated genes), identified using the DESeq2 R package. (B)

Distribution of differentially expressed transcript isoforms contained in genes without expression changes, identified using Cuffdiff. Only the isoforms that have a $|FC| \geq 2$ were considered as differentially expressed. (C) Summary of the biologically relevant pathways among the top 50 significantly enriched pathways in KEGG enrichment analysis for amiloride-deregulated isoforms detected in KMS12-BM (left) and JJN3 (right) cell lines. Statistical significance of the enrichment is expressed as -log10 (Benjamini-Hochberg adjusted *p*-value). (D) Alternative splicing events in genes without expression changes were detected using rMATS and classified into five main types of pattern: skipped exon (SE), mutually exclusive exons (MXE), alternative 5' splice site (A5SS), alternative 3' splice site (A3SS), and retained introns (RIs). rMATS also calculates the difference in the ratio of these events between two conditions, producing a false discovery rate.

Figure 5. **Amiloride affects the pre-mRNA splicing machinery in myeloma cells *in vitro*, independently of *TP53* status.** H929 (*TP53* WT) and JJN3 (*TP53* null) cells were treated with increasing concentrations of amiloride. SC35-staining nuclear speckles were detected by immunofluorescence after 24 h. Cell viability was analyzed by CellTiter-Glo luminescent assays and expressed as the mean ± SD. Statistically significant differences between amiloride-treated and untreated cells are presented. *p* values were assessed by the two-sided Student's *t* test.

Figure 6. The p53 signaling pathway is activated in *TP53* WT and MUT, but not in p53-null MM cells. (A) MM1S, KMS12-BM, JJN3 and U-266 cells were treated with increasing concentrations of amiloride. mRNA levels of *BBC3 (PUMA), BAX, BAK1, CDKN1A (p21), CDKN1B, TNFRSF10B* and *FAS (CD95)*, were assessed by qRT-PCR 24 h after amiloride treatment. The results are shown as the magnitude of change between treated and untreated cells and correspond to the average of three experiments after normalization with 18S rRNA. Statistically significant differences between untreated and treated cell lines are represented as $^{**}p < 0.01$ and $^{*}p < 0.05$ (Student's t-test). (B) Cell

viability upon amiloride (KMS12-BM at 0.1 mM; H929 at 0.2 mM; JJN3 and U-266 at 0.3 mM), pifithrin-α (10 nM) or pifithrin-μ (2.5 nM) treatment was analyzed by CellTiter-Glo luminescent assays, 24 h after amiloride treatment. Results are the mean of at least three independent experiments. Asterisks indicate statistically significant differences between amiloride-treated cells and amiloride-pifithrin-α/μ-treated cells; $^{**}p < 0.01$, $^{*}p < 0.05$ and *N.S.* no significant (Student's t-test).

Figure 1

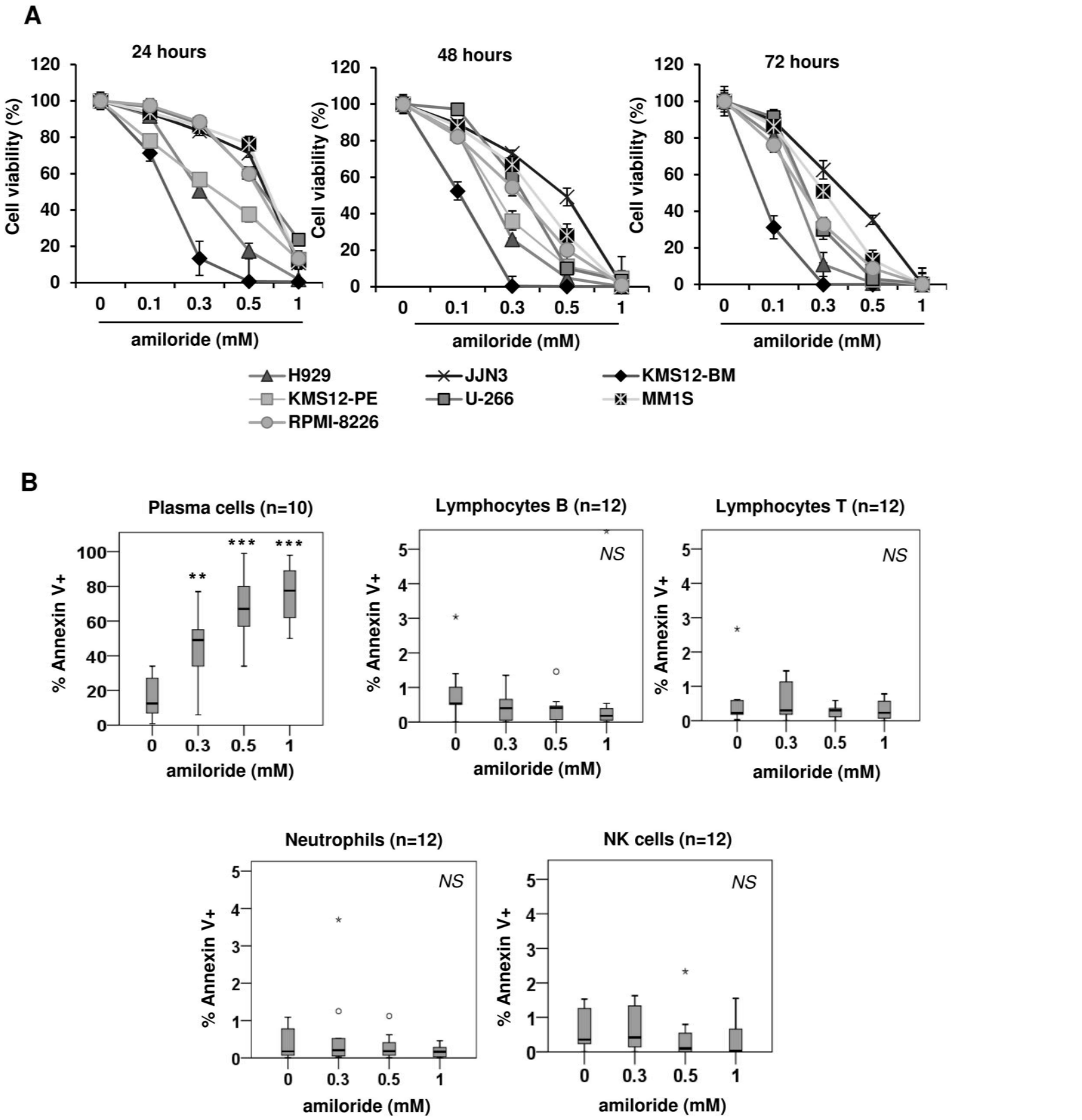
A
24 hours
48 hours
72 hours
Cell viability (%)
amiloride (mM)
H929
KMS12-PE
RPMI-8226
JJN3
U-266
KMS12-BM
MM1S
B
Plasma cells (n=10)
Lymphocytes B (n=12)
Lymphocytes T (n=12)
Neutrophils (n=12)
NK cells (n=12)
% Annexin V+
NS

C

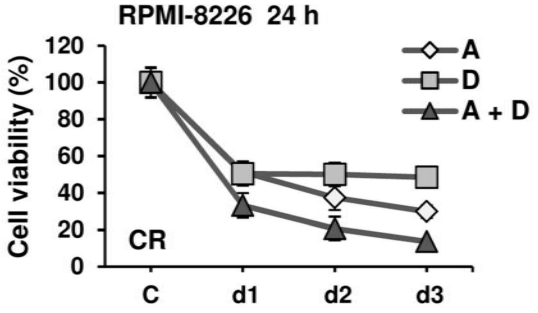

	Drugs concentration (μM)		CI
Drug	A	D	A + D
d1	133	6.7	0.528
d2	200	10	0.445
d3	300	15	0.427

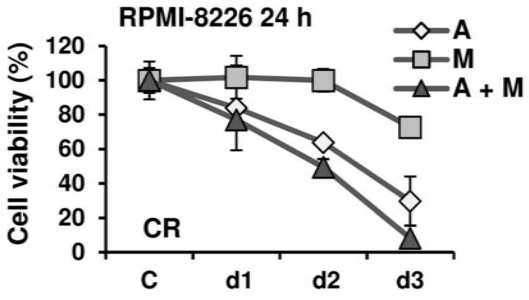

	Drugs concentration (μM)		CI
Drug	A	M	A + M
d1	100	4	0.868
d2	200	8	0.888
d3	400	16	0.492

D

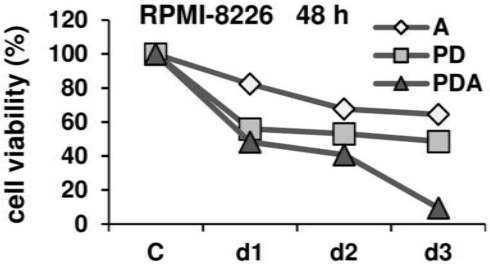

	Drugs concentration (μM)			CI
Drug	A	P	D	A + P + D
d1	50	0.125	1.25	0.330
d2	100	0.250	2.50	0.246
d3	200	0.500	5.00	0.018

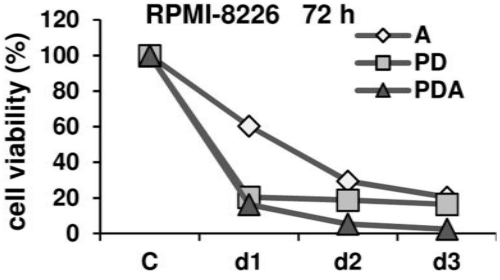

	Drugs concentration (μM)			CI
Drug	A	P	D	A + P + D
d1	50	0.125	1.25	0.458
d2	100	0.250	2.50	0.171
d3	200	0.500	5.00	0.185

E

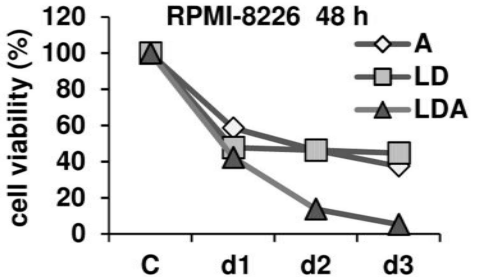

	Drugs concentration (μM)			CI
Drug	A	L	D	A + L + D
d1	50	0.125	1.25	0.431
d2	100	0.250	2.50	0.061
d3	200	0.500	5.00	0.022

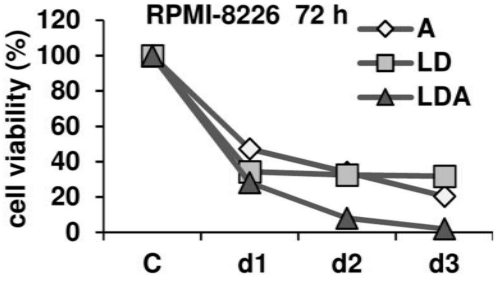

	Drugs concentration (μM)			CI
Drug	A	L	D	A + L + D
d1	50	0.125	1.25	0.426
d2	100	0.250	2.50	0.147
d3	200	0.500	5.00	0.058

Figure 2

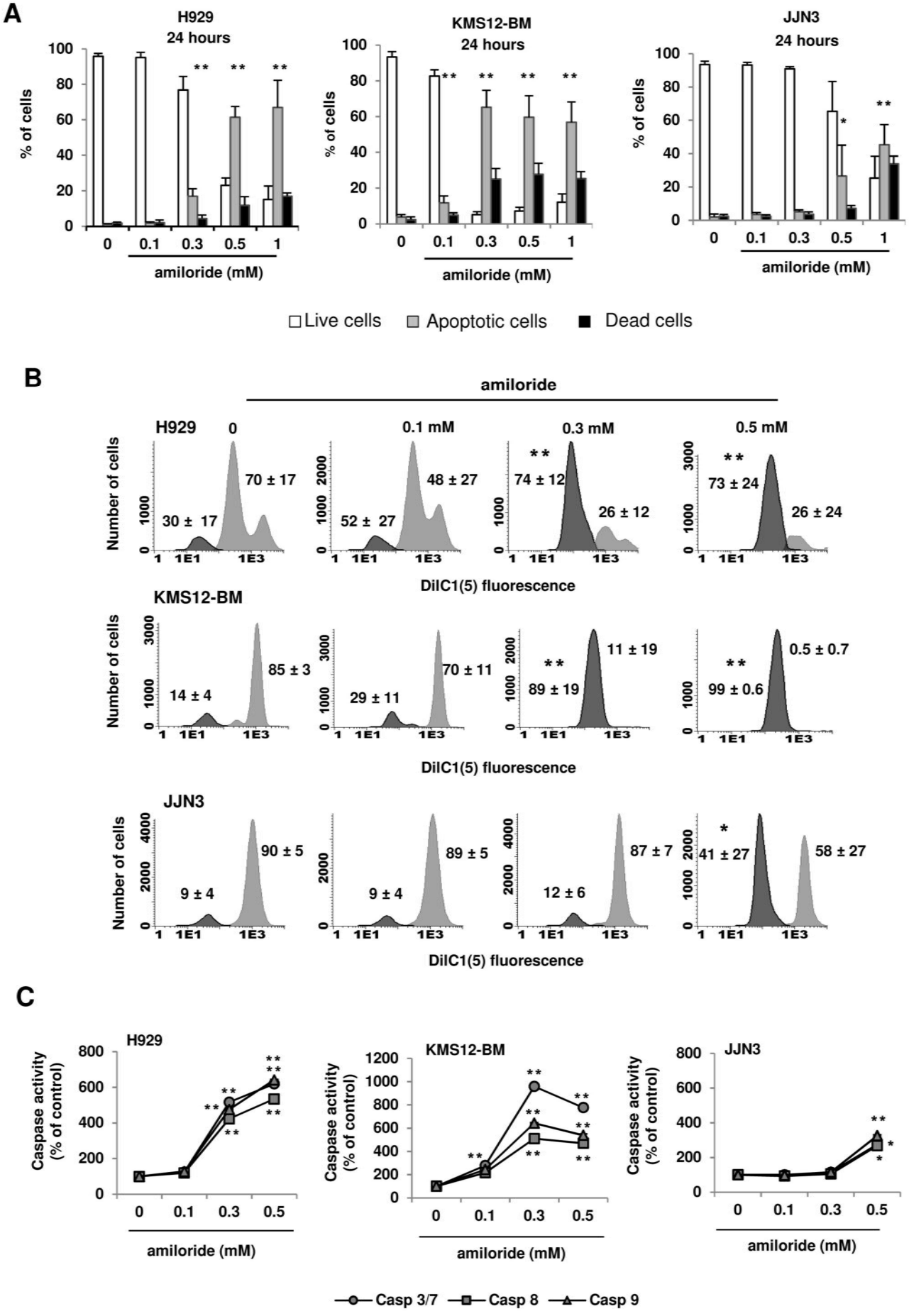
A
H929
24 hours
KMS12-BM
24 hours
JJN3
24 hours
% of cells
amiloride (mM)
0
0.1
0.3
0.5
1
Live cells
Apoptotic cells
Dead cells
B
amiloride
H929
0
0.1 mM
0.3 mM
0.5 mM
Number of cells
70 ± 17
30 ± 17
48 ± 27
52 ± 27
74 ± 12
26 ± 12
73 ± 24
26 ± 24
DiIC1(5) fluorescence
KMS12-BM
85 ± 3
14 ± 4
70 ± 11
29 ± 11
11 ± 19
89 ± 19
0.5 ± 0.7
99 ± 0.6
JJN3
90 ± 5
9 ± 4
89 ± 5
9 ± 4
87 ± 7
12 ± 6
41 ± 27
58 ± 27
C
H929
KMS12-BM
JJN3
Caspase activity (% of control)
amiloride (mM)
Casp 3/7
Casp 8
Casp 9

Figure 3

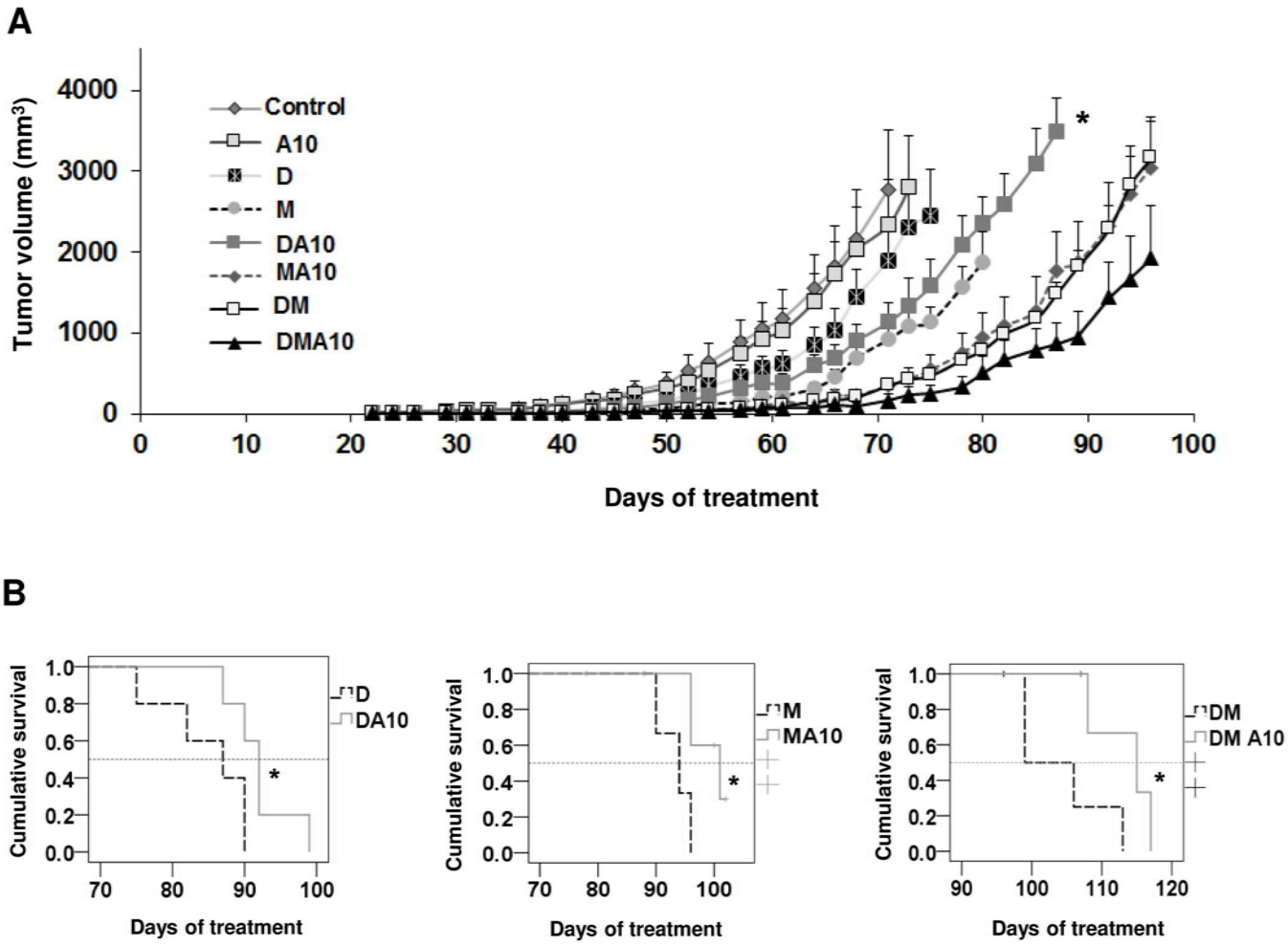
A
Tumor volume (mm3)
4000
3000
2000
1000
0
Control
A10
D
M
DA10
MA10
DM
DMA10
*
0
10
20
30
40
50
60
70
80
90
100
Days of treatment
B
Cumulative survival
1.0
0.8
0.6
0.4
0.2
0.0
D
DA10
*
70
80
90
100
Days of treatment
Cumulative survival
M
MA10
*
Days of treatment
Cumulative survival
DM
DM A10
*
90
100
110
120
Days of treatment

Figure 4

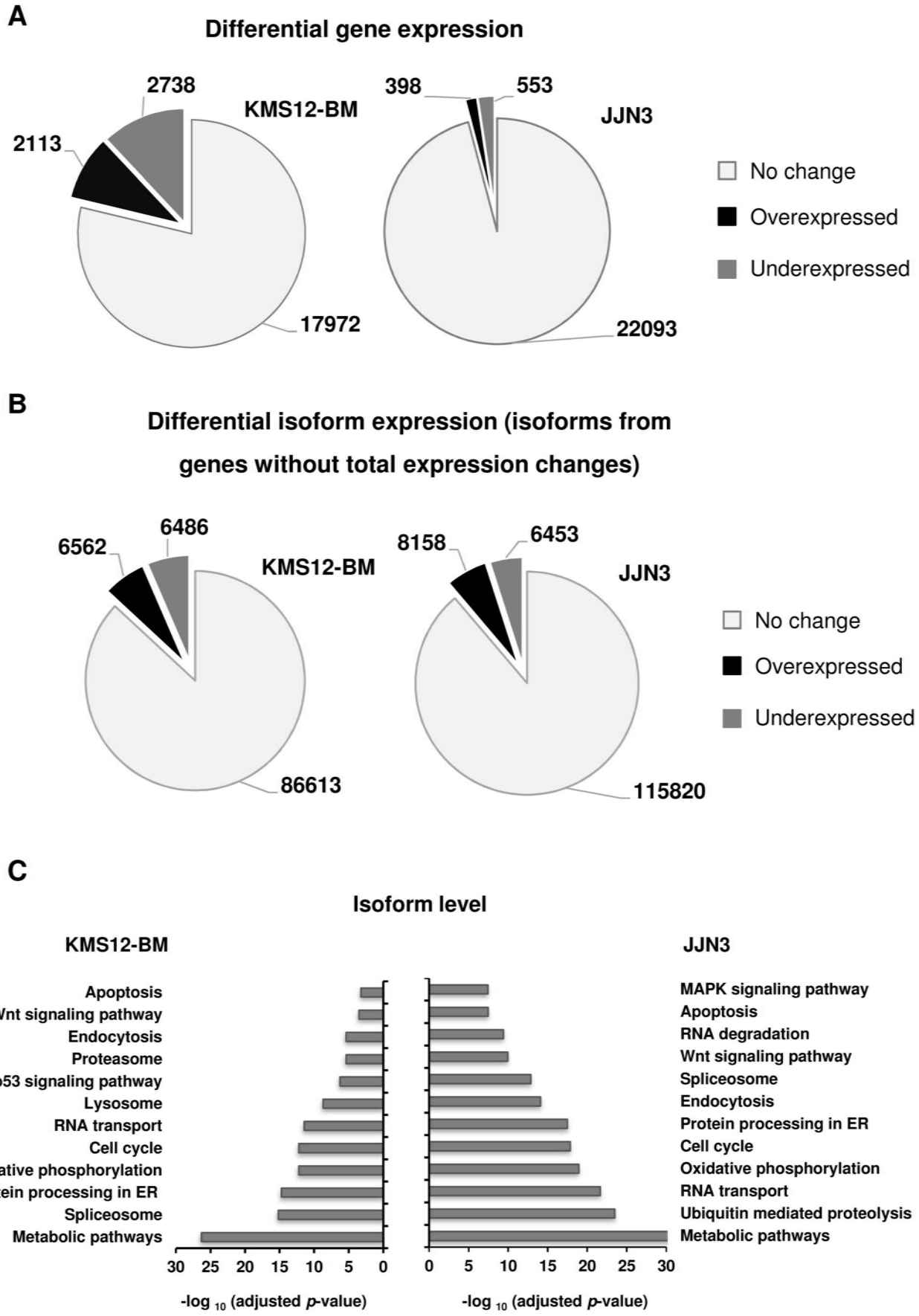
A
Differential gene expression
2738
2113
KMS12-BM
17972
398
553
JJN3
22093
No change
Overexpressed
Underexpressed
B
Differential isoform expression (isoforms from genes without total expression changes)
6562
6486
KMS12-BM
86613
8158
6453
JJN3
115820
No change
Overexpressed
Underexpressed
C
Isoform level
KMS12-BM
Apoptosis
Wnt signaling pathway
Endocytosis
Proteasome
p53 signaling pathway
Lysosome
RNA transport
Cell cycle
Oxidative phosphorylation
Protein processing in ER
Spliceosome
Metabolic pathways
30 25 20 15 10 5 0
-log 10 (adjusted p-value)
JJN3
MAPK signaling pathway
Apoptosis
RNA degradation
Wnt signaling pathway
Spliceosome
Endocytosis
Protein processing in ER
Cell cycle
Oxidative phosphorylation
RNA transport
Ubiquitin mediated proteolysis
Metabolic pathways
0 5 10 15 20 25 30
-log 10 (adjusted p-value)

D

Significant alternative splicing events

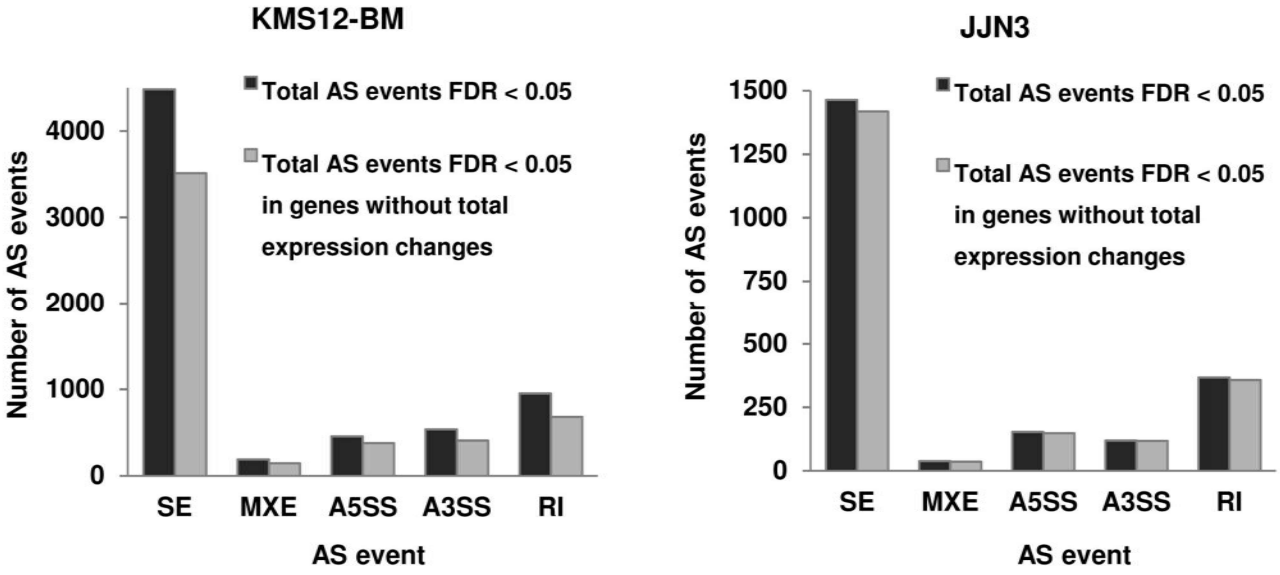

SE	MXE	A5SS	A3SS	RI		SE	MXE	A5SS	A3SS	RI
4484	192	458	539	953	**Total AS events FDR < 0.05**	1465	39	154	120	369
3512 **(78%)**	145 **(76%)**	379 **(83%)**	408 **(76%)**	684 **(72%)**	**Total AS events FDR < 0.05 in genes without total expression changes**	1419 **(97%)**	37 **(95%)**	148 **(96%)**	118 **(98%)**	358 **(97%)**

Figure 5

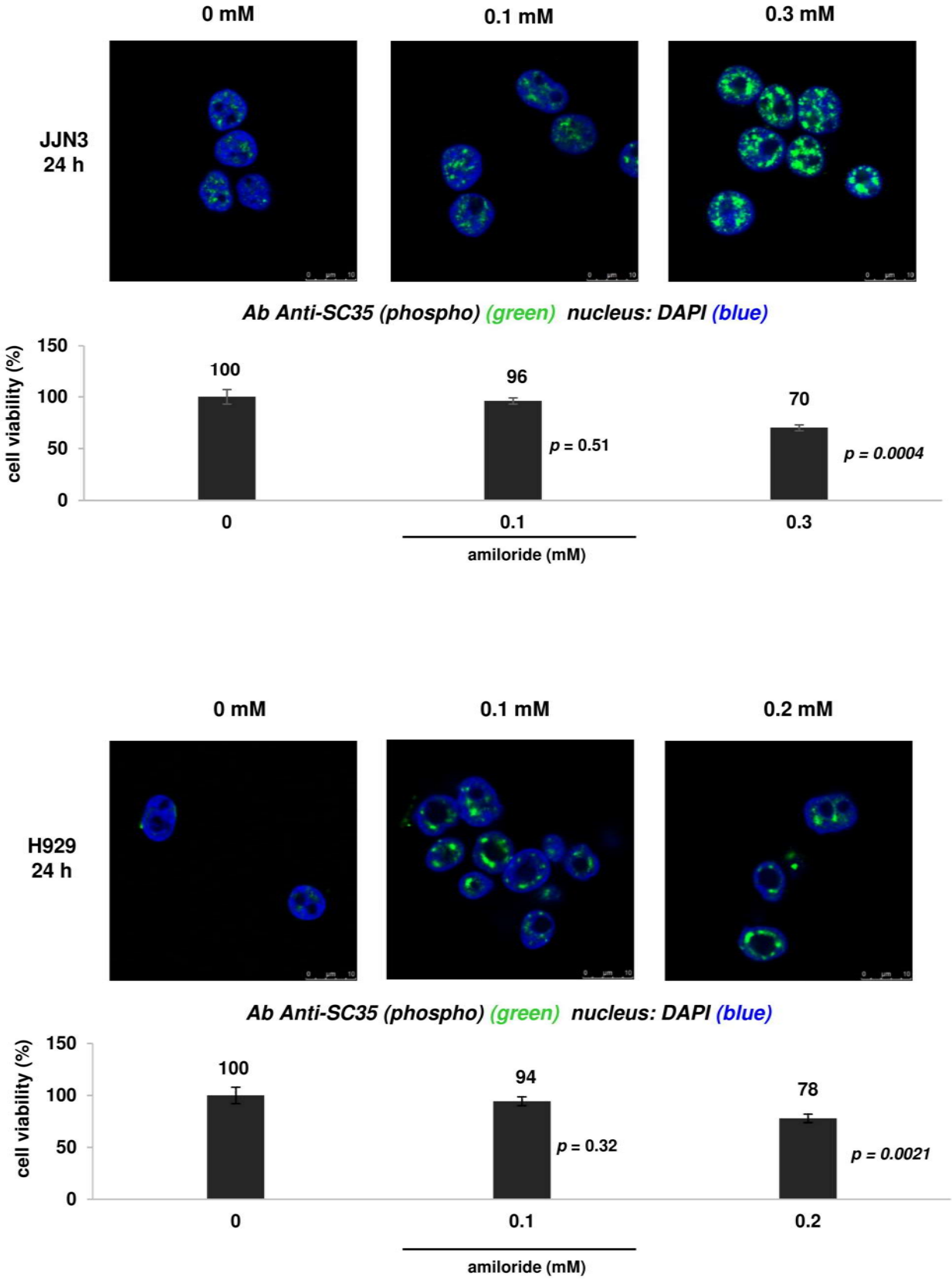
0 mM
0.1 mM
0.3 mM
JJN3
24 h
Ab Anti-SC35 (phospho) (green) nucleus: DAPI (blue)
cell viability (%)
150
100
50
0
100
96
70
p = 0.51
p = 0.0004
0
0.1
0.3
amiloride (mM)
0 mM
0.1 mM
0.2 mM
H929
24 h
Ab Anti-SC35 (phospho) (green) nucleus: DAPI (blue)
cell viability (%)
150
100
50
0
100
94
78
p = 0.32
p = 0.0021
0
0.1
0.2
amiloride (mM)

Figure 6

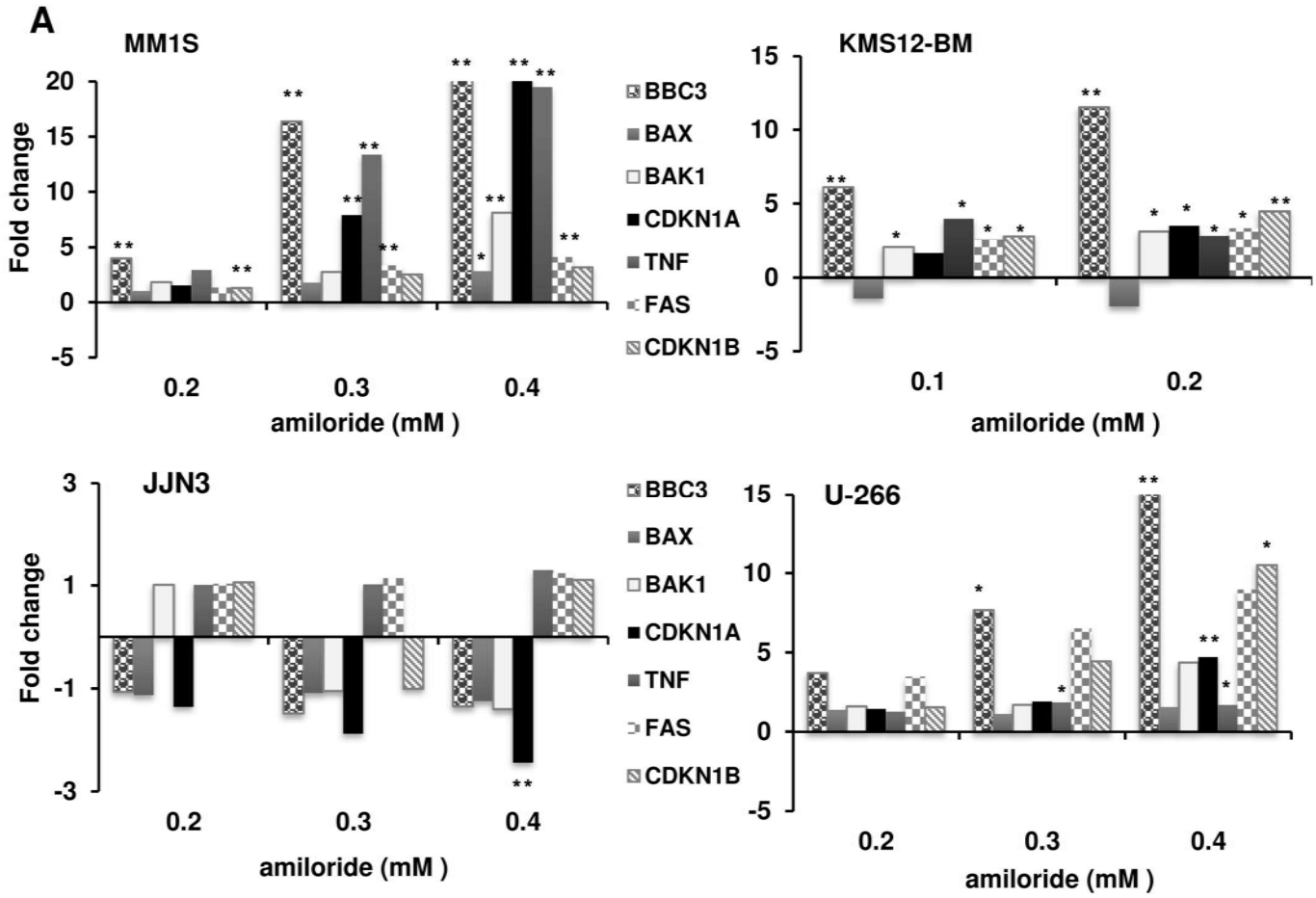
A
MM1S
Fold change
amiloride (mM)
0.2
0.3
0.4
BBC3
BAX
BAK1
CDKN1A
TNF
FAS
CDKN1B
KMS12-BM
0.1
0.2
JJN3
U-266

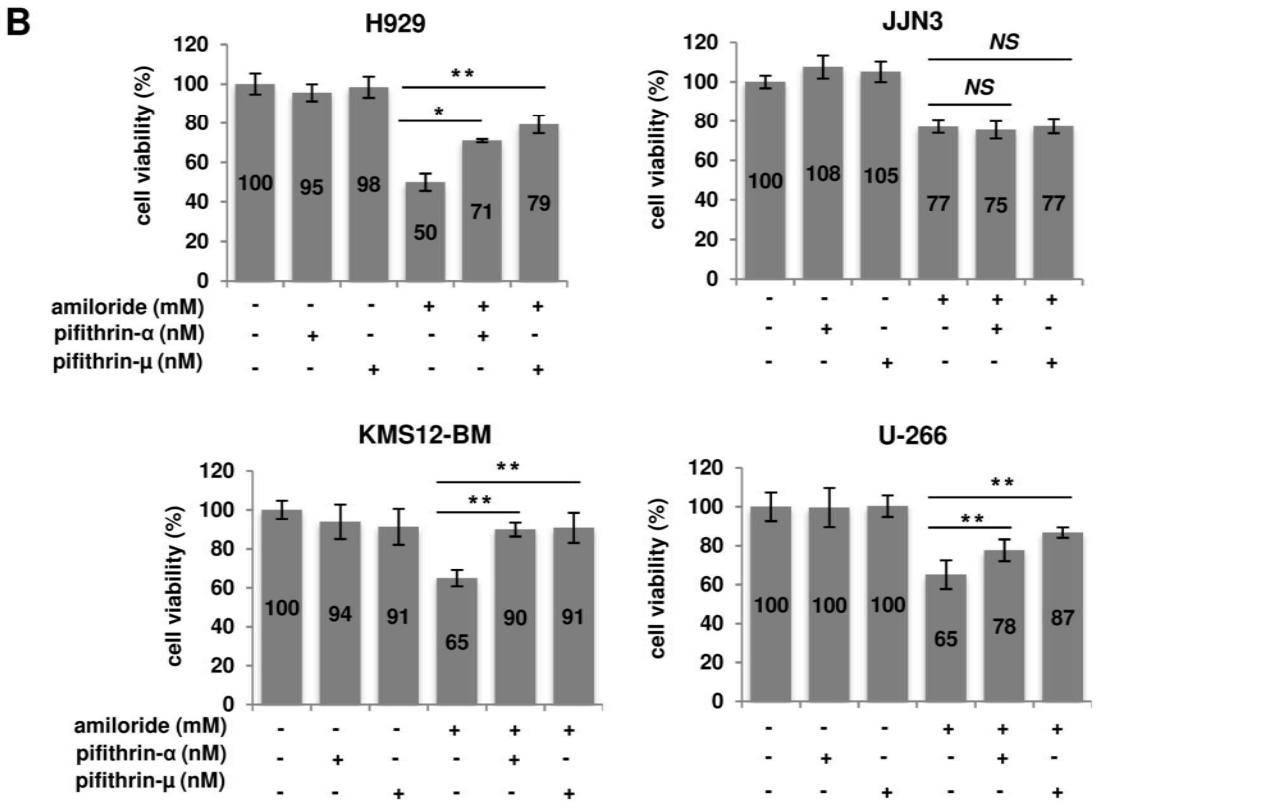
B
H929
JJN3
KMS12-BM
U-266
cell viability (%)
NS
amiloride (mM)
pifithrin-α (nM)
pifithrin-μ (nM)